



A Theoretical Study on Radiation Shielding Characteristics of Magnetic Shielding Alloys, $Ni_{80}Fe_{15}Mo_5$ and $Ni_{77}Fe_{14}Cu_5Mo_4$, by Determining the Photon Attenuation Parameters in the Energy Range of 15keV-100GeV

Manyetik Kalkan Alaşımaları $Ni_{80}Fe_{15}Mo_5$ ve $Ni_{77}Fe_{14}Cu_5Mo_4$ 'ün 15keV-100GeV Enerji Aralığında Foton Zayıflatma Parametrelerini Belirleyerek Radyasyon Zırhlama Özellikleri Üzerine Teorik Bir Çalışma

Zeynep Aygun^{1,*} , Murat Aygün² 

¹Bitlis Eren University, Vocational School of Technical Sciences, Bitlis, Turkey

²Bitlis Eren University, Faculty of Arts and Science, Department of Physics, Bitlis, Turkey

Abstract

In this study, we aimed to calculate photon-matter interaction parameters of $Ni_{80}Fe_{15}Mo_5$ and $Ni_{77}Fe_{14}Cu_5Mo_4$, which are known as magnetic shielding alloys. The parameters were determined by using Phy-X/PSD software. The radiation attenuation parameters such as mass attenuation coefficient, linear attenuation coefficient, effective atomic number, half-value layer, tenth-value layer, total atomic cross section and total electronic cross section were calculated between the photon energies 15keV and 100GeV in order to determine the radiation shielding potentials of the alloys. The shielding potentials of the alloys were compared with those of widely used shielding materials reported before.

Keywords: Radiation attenuation parameters, Radiation shielding, Magnetic shielding alloys

Öz

Bu çalışmada, manyetik kalkan alaşımaları olarak bilinen $Ni_{80}Fe_{15}Mo_5$ ve $Ni_{77}Fe_{14}Cu_5Mo_4$ 'ün foton-madde etkileşim parametrelerini hesaplamayı amaçladık. Parametreler Phy-X / PSD yazılımı kullanılarak belirlendi. Alaşımaların 15keV ve 100GeV foton enerjileri arasında radyasyon zırhlama potansiyellerinin belirlenmesi için kütle zayıflatma katsayısı, doğrusal zayıflatma katsayısı, efektif atom numarası, yarı kalınlık değeri, onda birine düşürme değeri, toplam atomik tesir kesiti ve toplam elektronik tesir kesiti gibi radyasyon zayıflatma parametreleri hesaplanmıştır. Alaşımaların zırhlama potansiyelleri, daha önce bildirilmiş yaygın olarak kullanılan zırhlama malzemelerinin potansiyelleriyle karşılaştırılmıştır.

Anahtar Kelimeler: Radyasyon zayıflatma katsayısı, Radyasyon zırhlama, Manyetik zırhlama alaşımaları


1. Introduction

Recently, there has been an enormous interest in researches including the determination of materials which have radiation shielding potentials due to the common applications of radiation in people's daily lives. By evaluation of the radiation attenuation parameters, we can have significant knowledge about the radiation shielding ability of the materials (Mann et al. 2013, Issa and Mostafa 2017, Kulali 2020, Alım 2020a). Some simulation codes and programs are widely used in order to determine the

radiation shielding parameters of different materials. Demir et al. (2013) investigated mass attenuation coefficients of water, concrete and bakelite at different energies by using the FLUKA Monte Carlo code. Photon attenuation parameters of some tissues by Geant4 simulation was studied by Arslan (2019). Radiation shielding properties of lanthanum oxide added waste soda-lime glass were studied via XCOM software by Akkurt et al. (2020). Tekin et al. (2020) reported the gamma-photon attenuation properties of newly developed molybdenum reinforced bismuth borate glasses by using MCNPX simulation code and XCOM program. Phy-X/PSD software recently developed by Sakar et al. (2020) is one of the codes which can be used for calculation of radiation shielding parameters of materials.

*Corresponding author: zeynep.yarbasi@gmail.com; zaygun@beu.edu.tr

Zeynep Aygun  orcid.org/0000-0002-2979-0283

Murat Aygün  orcid.org/0000-0002-4276-3511

Many studies have been carried out for determination of the parameters of compounds, glasses and alloys etc. at several photon energies before (Han and Demir 2009a, Han and Demir 2010, Yılmaz et al. 2016, Alim 2020b, Akkurt and Tekin 2020). Among the alloys, the high-nickel based alloys have high initial and maximum permeabilities, low coercivity and very low hysteresis losses. Additions of 4 to 5% Mo, or of copper and chromium to nickel-based NiFe alloys, improves the permeability (Aygun 2018, Oleksakova et al. 2020). Ni₈₀Fe₁₅Mo₅ and Ni₇₇Fe₁₄Cu₅Mo₄ soft magnetic alloys, known as magnetic shielding alloys (MSA), are used in resonance devices, superconducting circuits, electric transformer, storage disks, magnetic phonographs etc. Some of the photon attenuation parameters of Ni₇₇Fe₁₄Cu₅Mo₄ alloy were investigated for some energies before (Alim et al. 2019). To the best of our knowledge, the radiation shielding capabilities of Ni₈₀Fe₁₅Mo₅ and Ni₇₇Fe₁₄Cu₅Mo₄ alloys for the energies between 15keV and 100GeV have not been studied, yet. For this reason, in this study, we aimed to determine the mass attenuation coefficient (MAC), linear attenuation coefficient (LAC), effective atomic number (Z_{eff}), half-value layer (HVL), tenth-value layer (TVL), total atomic cross section (ACS) and total electronic cross section (ECS) parameters and radiation shielding features of Ni₈₀Fe₁₅Mo₅ and Ni₇₇Fe₁₄Cu₅Mo₄ in a wide energy range by using Phy-X/PSD software.

2. Materials and Methods

In the study, we obtained the Ni₈₀Fe₁₅Mo₅ and Ni₇₇Fe₁₄Cu₅Mo₄ alloys in the form of foil from Goodfellow Corporation commercially. The density of used alloys is 8.8 g/cm³.

The MAC is a quantity that defines the interaction possibility between gamma photons and the mass per unit area for a particular medium and can be calculated by the Beer-Lambert formulated as:

$$I = I_0 e^{-\mu t} \quad (1)$$

$$\mu_m = \frac{\mu}{\rho} = \ln(I_0/I) / \rho t = \ln(I_0/I) / t_m \quad (2)$$

where I_0 and I are incident and attenuated photon intensities, ρ (g/cm³) is the density of material, μ_m (cm²/g) and μ (cm⁻¹) are mass and linear attenuation coefficients, t_m (g/cm²) and t (cm) are sample mass thickness (the mass per unit area) and the thickness, respectively.

If the sample has various elements, we can write the total mass attenuation coefficient for any compound as follows (Jackson and Hawkes 1981);

$$\mu/\rho = \sum_i w_i (\mu/\rho)_i \quad (3)$$

where w_i and $(\mu/\rho)_i$ are the weight fraction and the mass attenuation coefficient of the i th constituent element, respectively.

The total atomic cross-section (σ_a) for any sample can be calculated using the equation formulated as;

$$ACS = \sigma_a = \frac{N}{N_A} (\mu/\rho) \quad (4)$$

where N_A and N respectively are the Avogadro's number and the atomic mass of materials.

The total electronic cross-section (σ_e) is formulated the following equation (Han and Demir 2009a);

$$ECS = \sigma_e = \frac{\sigma_a}{Z_{eff}} \quad (5)$$

By using the Equations (4) and (5), we can find the effective atomic number, Z_{eff} , of the material as follows;

$$Z_{eff} = \frac{\sigma_a}{\sigma_e} \quad (6)$$

We can calculate the effective electron number, N_{eff} , as follows (Han and Demir 2009b),

$$N_{eff} = \frac{\mu_m}{\sigma_e} \quad (7)$$

HVL and TVL are the thicknesses parameters that are the used to reduce the radiation intensities by one half and one tenth, respectively. MFP is the average distance at which a photon travels through the material between two interactions. The μ is used to obtain the parameters given by

$$HVL = \frac{\ln(2)}{\mu} \quad (8)$$

$$MFP = \frac{1}{\mu} \quad (9)$$

$$TVL = \frac{\ln 10}{\mu} \quad (10)$$

Effective conductivity (C_{eff}) of materials can be given by the following equation (Manjunatha 2017):

$$C_{eff} = \left(\frac{N_{eff} \rho e^2 \tau}{m_e} \right) 10^3 \quad (11)$$

where m_e (kg) and e (C) are mass and charge of electron, respectively.

3. Results and Discussion

Variations of the calculated MAC values of the soft magnetic alloys, Ni₈₀Fe₁₅Mo₅ and Ni₇₇Fe₁₄Cu₅Mo₄, versus photon

energies (15keV-100GeV) are shown in Figure 1A. In the low energy region (1-100keV) where the photoelectric process is predominant, MAC values decreased sharply with increasing energy. In the intermediate energy region (100keV-5MeV) where the Compton scattering is dominant, MAC values slightly changed. Above 5MeV, the Pair production process starts and an increase in MAC

values was observed with increasing energy (Kurudirek et al. 2009, Alim 2020a). We also calculated MAC values of the alloys by XCOM code reported by Berger and Hubbell (1987) to see the agreement of the values determined by Phy-X/PSD. It was observed that the obtained results are in good agreement as given in Table 1.

Table 1. MAC values of Ni₈₀Fe₁₅Mo₅ and Ni₇₇Fe₁₄Cu₅Mo₄ alloys determined by XCOM and Phy-X/PSD.

Energy MeV	Ni ₈₀ Fe ₁₅ Mo ₅		Ni ₇₇ Fe ₁₄ Cu ₅ Mo ₄	
	Phy-X/PSD cm ² /g	XCOM cm ² /g	Phy-X/PSD cm ² /g	XCOM cm ² /g
1.50E-02	65.52	66.60	66.49	67.40
2.00E-02	35.07	33.60	34.46	33.30
3.00E-02	11.45	10.90	11.22	10.80
4.00E-02	5.130	4.870	5.021	4.810
5.00E-02	2.767	2.630	2.706	2.590
6.00E-02	1.689	1.600	1.652	1.580
8.00E-02	0.810	0.772	0.793	0.762
1.00E-01	0.486	0.466	0.477	0.461
1.50E-01	0.233	0.227	0.230	0.225
2.00E-01	0.163	0.161	0.162	0.160
3.00E-01	0.116	0.116	0.116	0.115
4.00E-01	0.098	0.097	0.097	0.097
5.00E-01	0.087	0.086	0.087	0.086
6.00E-01	0.079	0.079	0.079	0.078
8.00E-01	0.068	0.068	0.068	0.068
1.00E+00	0.061	0.061	0.061	0.061
1.50E+00	0.050	0.049	0.050	0.049
2.00E+00	0.044	0.043	0.043	0.043
3.00E+00	0.037	0.037	0.037	0.037
4.00E+00	0.034	0.034	0.034	0.034
5.00E+00	0.033	0.032	0.033	0.032
6.00E+00	0.032	0.032	0.032	0.031
7.00E+00	0.032	0.031	0.032	0.031
8.00E+00	0.032	0.031	0.032	0.031
9.00E+00	0.032	0.031	0.032	0.031
1.00E+01	0.032	0.031	0.032	0.031
1.10E+01	0.032	0.032	0.032	0.032
1.20E+01	0.032	0.032	0.032	0.032
1.30E+01	0.033	0.032	0.033	0.032
1.40E+01	0.033	0.032	0.033	0.032
1.50E+01	0.033	0.033	0.033	0.033
1.60E+01	0.034	0.033	0.034	0.033
1.80E+01	0.034	0.034	0.034	0.034

Table 1. Cont.

Energy MeV	$Ni_{80}Fe_{15}Mo_5$		$Ni_{77}Fe_{14}Cu_5Mo_4$	
	Phy-X/PSD cm^2/g	XCOM cm^2/g	Phy-X/PSD cm^2/g	XCOM cm^2/g
2.00E+01	0.035	0.034	0.035	0.034
2.20E+01	0.036	0.035	0.036	0.035
2.40E+01	0.036	0.036	0.036	0.035
2.60E+01	0.037	0.036	0.037	0.036
2.80E+01	0.037	0.037	0.037	0.037
3.00E+01	0.038	0.037	0.038	0.037
4.00E+01	0.040	0.039	0.040	0.039
5.00E+01	0.042	0.041	0.042	0.041
6.00E+01	0.044	0.043	0.043	0.043
8.00E+01	0.046	0.045	0.046	0.045
1.00E+02	0.048	0.047	0.048	0.047
1.50E+02	0.051	0.050	0.050	0.050
2.00E+02	0.053	0.052	0.052	0.051
3.00E+02	0.055	0.054	0.054	0.054
4.00E+02	0.056	0.055	0.056	0.055
5.00E+02	0.057	0.056	0.057	0.056
6.00E+02	0.057	0.056	0.057	0.056
8.00E+02	0.058	0.057	0.058	0.057
1.00E+03	0.059	0.058	0.058	0.058
1.50E+03	0.060	0.059	0.059	0.058
2.00E+03	0.060	0.059	0.060	0.059
3.00E+03	0.060	0.059	0.060	0.059
4.00E+03	0.061	0.060	0.060	0.059
5.00E+03	0.061	0.060	0.061	0.060
6.00E+03	0.061	0.060	0.061	0.060
8.00E+03	0.061	0.060	0.061	0.060
1.00E+04	0.061	0.060	0.061	0.060
1.50E+04	0.061	0.060	0.061	0.060
2.00E+04	0.061	0.060	0.061	0.060
3.00E+04	0.061	0.060	0.061	0.060
4.00E+04	0.061	0.060	0.061	0.060
5.00E+04	0.061	0.060	0.061	0.060
6.00E+04	0.062	0.060	0.061	0.060
8.00E+04	0.062	0.061	0.061	0.060
1.00E+05	0.062	0.061	0.061	0.060

LAC is one of the parameters for defining the photon-matter interaction, but it is not sufficient. The value of LAC depends on both MAC and density of compound. Additionally, it is evaluated to calculate MAC, HVL and MFP shielding parameters. Dependence of the calculated LAC values versus photon energies (15keV-100GeV) is

shown in Figure 1B. Due to the density effect, differences of LAC values are greater than those of MAC values. It was obtained that the MAC and LAC values of both alloys were very near to each other for the given energies. In low energies, MAC values of $Ni_{80}Fe_{15}Mo_5$ alloy are slightly bigger than those of $Ni_{77}Fe_{14}Cu_5Mo_4$, it can be

said that $\text{Ni}_{80}\text{Fe}_{15}\text{Mo}_5$ has more absorption feature than $\text{Ni}_{77}\text{Fe}_{14}\text{Cu}_5\text{Mo}_4$. According to the obtained higher MAC and LAC values of the $\text{Ni}_{80}\text{Fe}_{15}\text{Mo}_5$ and $\text{Ni}_{77}\text{Fe}_{14}\text{Cu}_5\text{Mo}_4$, it can be said that the alloys have more shielding abilities than the widely used shielding materials (ordinary concrete, hematite-serpenite, basalt-magnetite, ilmenite-limonite, steel-scrap, ilmenite concrete and steel-magnetite) reported by Bashter (1997). It was also observed that the determined MAC values of the alloys are higher than those of the Ag_2O doped boro-tellurite glasses obtained by Alim (2020a).

The interaction possibility of per atom and per electron in a unit volume of any material is given by ACS and ECS, respectively. In Figure 2A, B; changing of ACS and ECS values as a function of incident photon energies are given. The alloy with higher ACS and ECS values can be evaluated as better shielding alloy (Alim 2020a). According to the results, due to the ACS and ECS values of the alloys are very close to each other, the shielding potential cannot be determined clearly by ACS and ECS parameters.

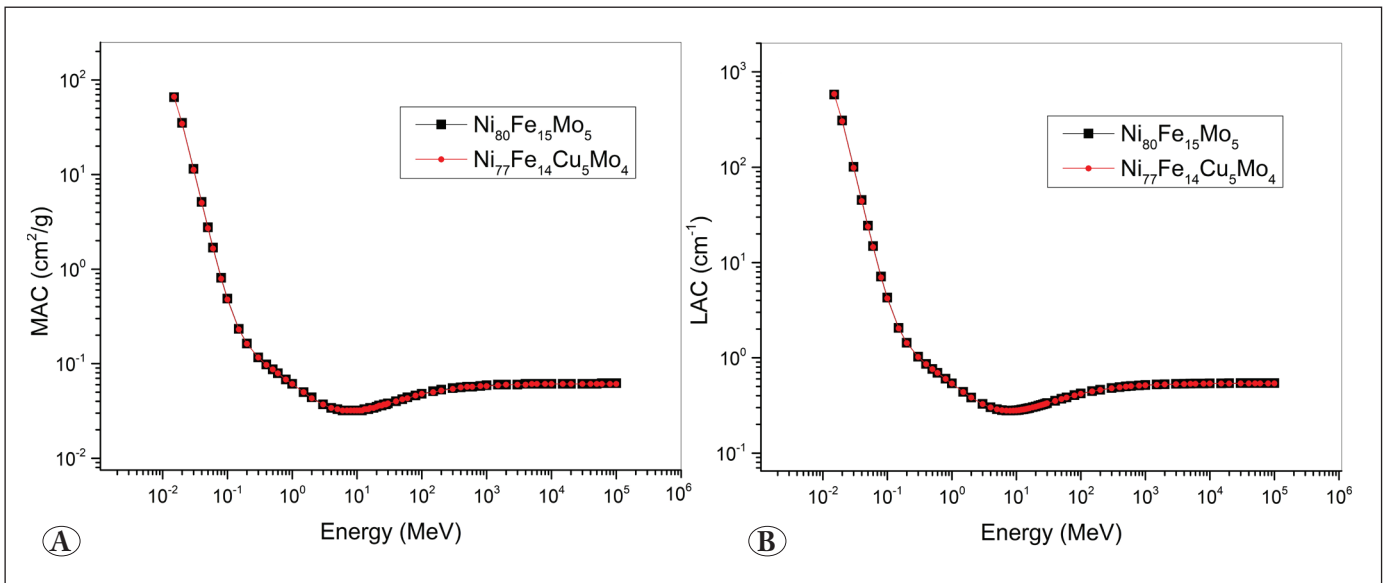


Figure 1. The changes of MAC (A) and LAC (B) as a function of incident photon energy.

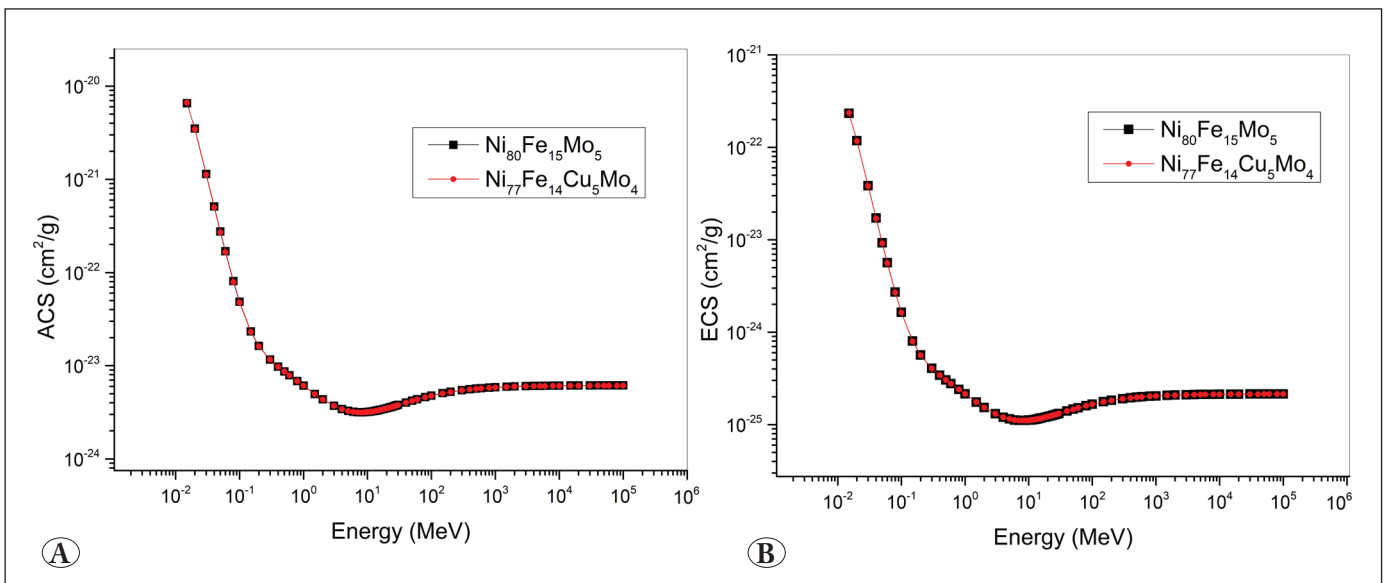


Figure 2. Dependence of ACS (A) and ECS (B) versus incident photon energy.

The HVL and TVL are the parameters for understanding of the penetration ability of the radiations in materials (Akkaş 2016). HVL and TVL parameters changing with the incident photon energies are given in Figure 3A, B. It is preferred to have low HVL and TVL values in the high energy regions for better shielding property. Although, HVL and TVL values of the alloys are very close to each other, lower HVL and TVL values were obtained for $\text{Ni}_{80}\text{Fe}_{15}\text{Mo}_5$ at high energies.

The energy dependence of MFP and Z_{eff} are given in Figure 4A, B. Like HVL and TVL, the same conclusion can be

evaluated for MFP values of the alloys. In the middle energy region where Compton scattering is dominant, most photons are more likely to be scattered. Therefore, their absorption probabilities are lower and hence thicker materials are required and photons have longer MFP. In the low energy region due to the photoelectric effect, maximum Z_{eff} values were obtained. By increasing energy, these values decreased sharply. Then the values gradually increased and remained constant in the high energy region. Due to the higher Z_{eff} values of $\text{Ni}_{80}\text{Fe}_{15}\text{Mo}_5$ than those of $\text{Ni}_{77}\text{Fe}_{14}\text{Cu}_5\text{Mo}_4$, it can be said that $\text{Ni}_{80}\text{Fe}_{15}\text{Mo}_5$

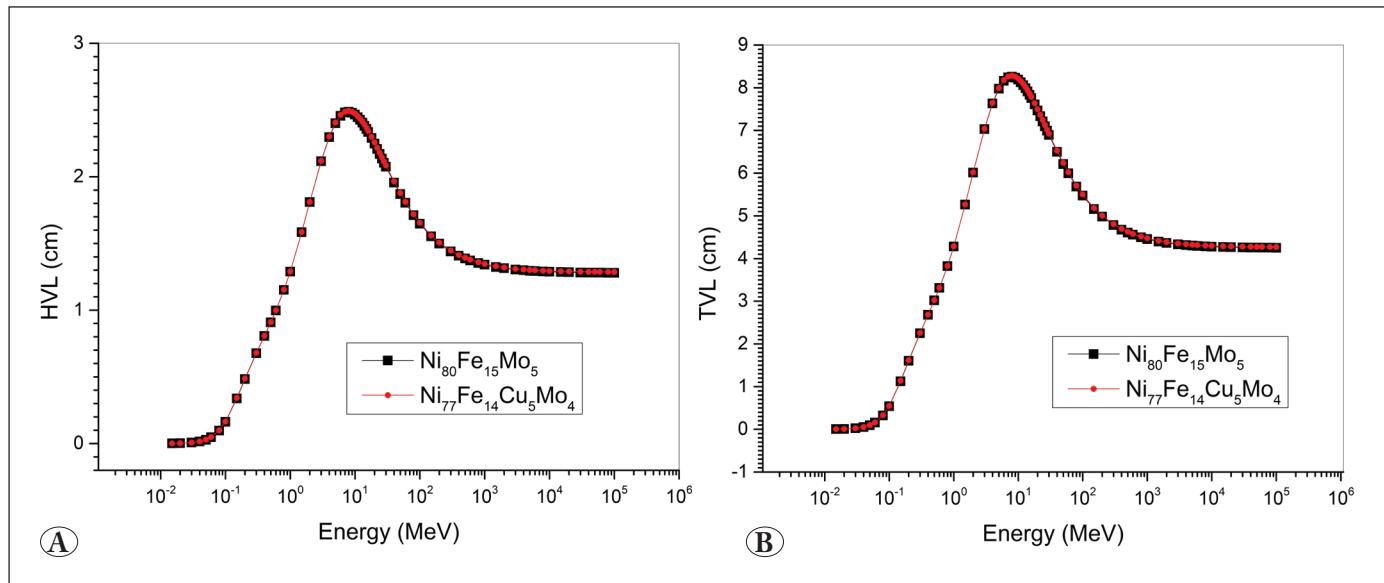


Figure 3. The variations of HVL (A) and TVL (B) as a function of incident photon energy.

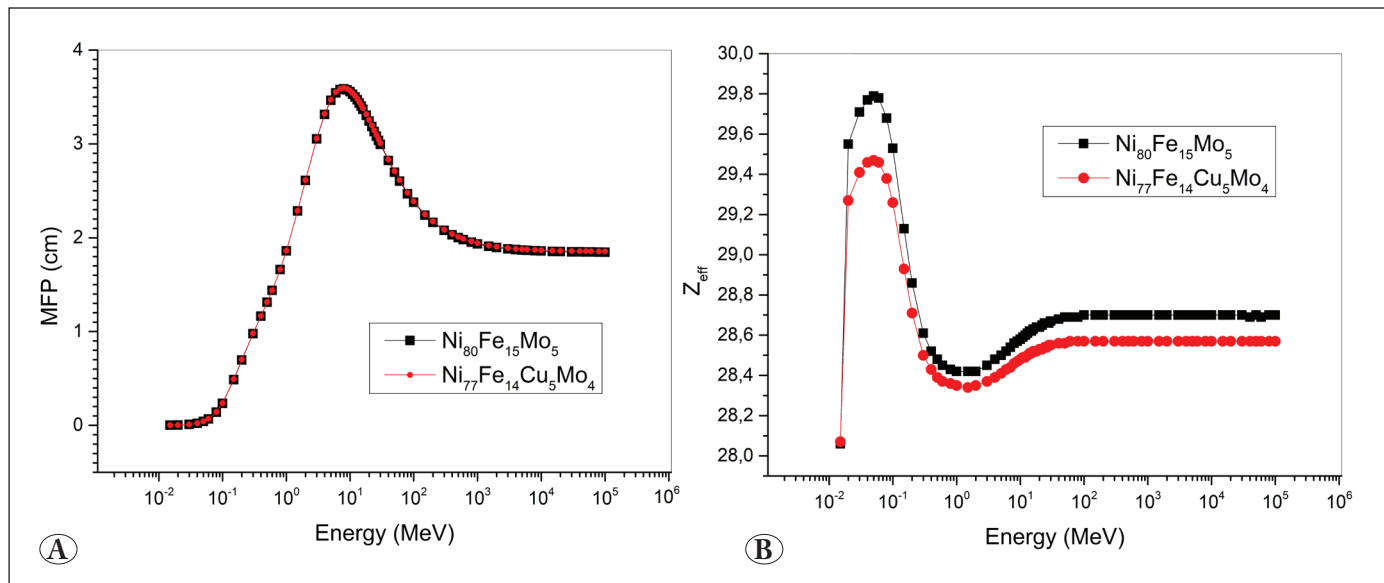


Figure 4. The changes of MFP (A) and Z_{eff} (B) as a function of incident photon energy.

shows higher shielding potential. The obtained Z_{eff} values of Ni₈₀Fe₁₅Mo₅ and Ni₇₇Fe₁₄Cu₅Mo₄, are also higher than the Z_{eff} values of RS 253 glass, ordinary concrete, hematite-serpenite and basalt-magnetite calculated by Alım (2020a) and hence, the alloys show more shielding property than the previously reported materials.

In conclusion, radiation-matter interaction parameters of soft magnetic alloys, Ni₈₀Fe₁₅Mo₅ and Ni₇₇Fe₁₄Cu₅Mo₄, were calculated by Phy-X / PSD code in the range of 15keV-100GeV to determine the radiation shielding capabilities in the present study. A good agreement was observed between MAC values of the alloys obtained by Phy-X/PSD and XCOM softwares. According to the obtained results, it was concluded that although, the parameters of the studied soft magnetic alloys have near values to each other, Ni₈₀Fe₁₅Mo₅ has higher shielding potential compared to Ni₇₇Fe₁₄Cu₅Mo₄. It can be also mentioned that both of the alloys show higher shielding capability than the commonly used shielding materials such as ordinary concrete, hematite-serpenite, basalt-magnetite, ilmenite-limonite, steel-scrap, ilmenite concrete and steel-magnetite.

Conflict of Interest

No conflict of interest was declared by the authors.

4. References

- Akkaş, A. 2016.** Determination of the Tenth and Half Value Layer Thickness of Concretes with Different Densities. *Acta Phys. Polonica A*, 129: 770-772. <https://doi.org/10.12693/APhysPolA.129.770>
- Akkurt, I. and Tekin, H.O. 2020.** Radiological parameters of bismuth oxide glasses using the Phy-X/PSD software. *Emerging Mater. Res.*, 9: 1020-1027. <https://doi.org/10.1680/jemmr.20.00209>
- Akkurt, I., Gunoglu, K., Kurtulus, R. and Kavas, T. 2020.** X-ray shielding parameters of lanthanum oxide added waste soda-lime glass. *X-Ray Spectrom.*, 1-12. <https://doi.org/10.1002/xrs.3210>
- Alım, B., Şakar, E., Özpolat, ÖF., Han, I. and Demir, L. 2019.** Determination of Gamma Photon Protection Capability of Ni₇₇Fe₁₄Cu₅Mo₄: A Magnetic Shielding Alloy. 4th Inter. Conf. Adv. Natural Appl. Sci. Phys., 266-276.
- Alım, B. 2020a.** Determination of Radiation Protection Features of the Ag₂O Doped Boro-Tellurite Glasses Using Phy-X / PSD Software. *J. Inst. Sci. Tech.*, 10(1): 202-213. <https://doi.org/10.21597/jist.640027>
- Alım, B. 2020b.** A comprehensive study on radiation shielding characteristics of Tin-Silver, Manganin-R, Hastelloy-B, Hastelloy-X and Dilver-P alloys. *Appl. Phys. A*, 126:262. <https://doi.org/10.1007/s00339-020-3442-7>
- Arslan, H. 2019.** Photon attenuation parameters for some tissues from Geant4 simulation, theoretical calculations and experimental data: a comparative study. *Nucl. Sci. Tech.* 30: 1-10. <https://doi.org/10.1007/s41365-019-0617-z>
- Aygun, Z. 2018.** Application of Spectroscopic Methods for Analysis of Ni-Based Alloys (Ni% ≥70). *Cumburiyet Sci. J.*, 39: 144-151. <https://doi.org/10.17776/csj.405681>
- Bashter, II. 1997.** Calculation of radiation attenuation coefficients for shielding concretes. *Ann. Nucl. Energy*, 24(17): 1389-1401. [https://doi.org/10.1016/S0306-4549\(97\)00003-0](https://doi.org/10.1016/S0306-4549(97)00003-0)
- Berger, MJ., Hubbell, JH., 1987.** XCOM: Photon Cross Sections Database, Web Version 1.2. National Institute of Standards and Technology, Gaithersburg, MD 20899, USA available at. <http://physics.nist.gov/xcom>.
- Demir, N., Tarım, UA., Popovici, MA., Demirci, ZN., Gurler, O. and Akkurt, I. 2013.** Investigation of mass attenuation coefficients of water, concrete and bakelite at different energies using the FLUKA Monte Carlo code. *J. Radioanal. Nucl. Chem.*, 298:1303-1307. <https://doi.org/10.1007/s10967-013-2494-y>
- Han, I. and Demir, L. 2009a.** Determination of mass attenuation coefficients, effective atomic and electron numbers for Cr, Fe and Ni alloys at different energies. *Nucl. Instr. Methods B*, 267: 3-8. <https://doi.org/10.1016/j.nimb.2008.10.004>
- Han, I. and Demir, L. 2009b.** Studies on effective atomic numbers, electron densities from mass attenuation coefficients in TixCo1-x and CoxCu1-x alloys. *Nucl. Instr. Methods B*, 267: 3505-3510. <https://doi.org/10.1016/j.nimb.2009.08.022>
- Han, I. and Demir, L. 2010.** Studies on effective atomic numbers, electron densities and mass attenuation coefficients in Au alloys. *J. X-ray Sci. Tech.*, 18: 39-46. <https://doi.org/10.3233/XST-2010-0238>
- Jackson, DF. and Hawkes, DJ. 1981.** X-ray attenuation coefficients of elements and mixtures. *Phys. Reports*, 70: 169-233. [https://doi.org/10.1016/0370-1573\(81\)90014-4](https://doi.org/10.1016/0370-1573(81)90014-4)
- Issa, SAM. and Mostafa, AMA. 2017.** Effect of Bi₂O₃ in borate-tellurite-silicate glass system for development of gamma-rays shielding materials. *J. Alloys Comp.*, 695: 302-310. <https://doi.org/10.1016/j.jallcom.2016.10.207>
- Kulali, F. 2020.** Simulation studies on the radiological parameters of marble concrete. *Emerging Mater. Res.*, 9: 1341-1347. <https://doi.org/10.1680/jemmr.20.00307>

- Kurudirek, M., Türkmen, I. and Özdemir, Y. 2009.** A study of photon interaction in some building materials: High-volume admixture of blast furnace slag into Portland cement. *Radiat. Phys. Chem.*, 78: 751–759. <https://doi.org/10.1016/j.radphyschem.2009.03.070>
- Manjunatha, HC. 2017.** A study of gamma attenuation parameters in poly methyl methacrylate and Kapton. *Radiat. Phys. Chem.*, 137: 254–259. <https://doi.org/10.1016/j.radphyschem.2016.01.024>
- Mann, KS., Kaur, B., Sidhu, GS. and Kumar, A. 2013.** Investigations of some building materials for g-rays shielding effectiveness. *Radiat. Phys. Chem.*, 87: 16-25. <https://doi.org/10.1016/j.radphyschem.2013.02.012>
- Olekšáková, D., Kollár, P., Jakubcin, M., Slovenský, P., Bircáková, Z., Füzér, J., Fáberová, M. and Bureš, R. 2020.** Anhyseretic Magnetization for NiFeMo Soft Magnetic Compacted Powder. *Acta Phys. Polonica A*, 137: 899-891. <https://doi.org/10.12693/APhysPolA.137.889>
- Şakar, E., Özpolat, ÖF., Alim, B., Sayyed, MI. and Kurudirek, M. 2020.** Phy-X / PSD: Development of a user friendly online software for calculation of parameters relevant to radiation shielding and dosimetry. *Radiat. Phys. Chem.*, 166: 1-12. <https://doi.org/10.1016/j.radphyschem.2019.108496>
- Tekin, HO., Abouhaswa, AS., Kilicoglu, O., Issa, SAM., Akkurt, I. and Rammah, YS. 2020.** Fabrication, physical characteristic, and gamma-photon attenuation parameters of newly developed molybdenum reinforced bismuth borate glasses. *Phys. Scr.*, 95. <https://doi.org/10.1088/1402-4896/abbf6e>
- Yılmaz, D., Boydaş, E. and Cömert, E. 2016.** Determination of mass attenuation coefficients and effective atomic numbers for compounds of the 3d transition elements. *Radiat. Phys. Chem.*, 125: 65–68. <https://doi.org/10.1016/j.radphyschem.2016.03.014>